0026-895X/89/010134-08$02.00/0

MOLECULAR PHARMACOLOGY, 36:134-141

Interaction of [^{3}H]Dilazep at Nucleoside Transporter-Associated Binding Sites on S49 Mouse Lymphoma Cells

WENDY P. GATI and ALAN R. P. PATERSON

Cancer Research Group (McEachern Laboratory) and Department of Pharmacology, University of Alberta, Edmonton, Alberta, Canada T6G 2H7

Received July 11, 1988; Accepted March 2, 1989

SUMMARY

Dilazep, a tertiary amine that is >96% protonated at pH 7.4, is a potent inhibitor of facilitated diffusion (equilibrative) nucleoside transport (NT) in animal cells. In this study, saturable reversible binding of [^{3}H]dilazep was demonstrated at sites on S49 mouse lymphoma cells but not in AE_1 cells, an NT-deficient mutant of S49 cells. Mass law analysis of dilazep binding under equilibrium conditions revealed two saturable components, representing binding sites that differed about 50-fold in affinity for dilazep (K_d values of 0.21 and 10 nM). At pH 7.4, the low affinity sites were more abundant (B_{max}, 3.5×10^5 sites/cell) than the high affinity sites (B_{max}, 3.0×10^4 sites/cell). Binding of dilazep was pH dependent; at pH 9.0, binding at the high affinity sites predominated, whereas, at pH 5.0, the low affinity component predominated, suggesting that these components represented binding of nonprotonated and protonated dilazep molecules, respectively. Nitrobenzylthioinosine (NBMPR) and physostigmine selectively blocked binding of nonprotonated and protonated species of dilazep, respectively, at pH 7.4, yielding Scatchard plots that were similar to control plots obtained at pH 5.0 and 9.0. First-order plots of the dissociation of [^{3}H]dilazep-binding site complexes in the presence of excess nonradioactive dilazep at pH 7.4 were nonlinear and were resolved into rapid (rate constant, 3.4–4.7 min^{-1}) and slow (rate constant, 0.13–0.15 min^{-1}) components. In the presence of site-saturating concentrations of NBMPR or high concentrations of nucleoside permeants, dissociation of site-bound [^{3}H]dilazep was incomplete and only the slow component of dissociation was apparent (rate constant, 0.11–0.19 min^{-1}). The combined presence of nonradioactive dilazep and NBMPR yielded time courses of [^{3}H]dilazep-site dissociation equivalent to those obtained in the presence of nonradioactive dilazep alone. These results are consistent with a model in which protonated and nonprotonated species of dilazep bind at separate sites on S49 cells. The absence of both high and low affinity sites on AE_1 cells suggests that, in S49 cells, both populations of sites are associated with NT polypeptides. The high affinity sites that bind nonprotonated species of dilazep appear to overlap with NBMPR binding sites on these cells.

NT in animal cells occurs through both equilibrative (1–5) and concentrative, sodium-dependent (6–11) mechanisms. Equilibrative NT systems may be classified according to their sensitivity to inhibition by NBMPR and the presence or absence of binding sites for this inhibitor (2, 5, 12–15). Although NBMPR and congeners are potent inhibitors of equilibrative NT, other structurally unrelated agents are also potent NT inhibitors. The latter include dipyridamole (16–19), dilazep (20–23), hexobendine (23), and lidoflazine (19), all of which are recognized as vasodilatory substances. Dilazep and hexobendine are amphiphilic compounds that contain tertiary nitrogen atoms that are partially protonated in solution at pH 7.4 (24).

Inhibition of site-specific binding of NBMPR by dipyridamole (15, 25, 26), dilazep (15, 23, 26, 27), hexobendine (23, 26), and lidoflazine (26) has been reported. Studies with mammalian erythrocytes have led to the hypothesis that dipyridamole binds at membrane sites that overlap with NBMPR binding sites (17, 28).

Dilazep (1,4-bis-[3-(3,4,5-trimethoxybenzoyl-oxy)propyl] perhydro-1,4-diazepine) is one of the most potent of the non-nucleoside NT inhibitors. IC_{50} values for inhibition of NBMPR-sensitive equilibrative NT in human erythrocytes and in several lines of cultured cells range from 5 to 100 nM (20, 22, 23). Because of its high water solubility, dilazep dihydrochloride has been used as an NT quencher in inhibitor-stop procedures to rapidly terminate intervals of nucleoside influx (21, 22).

Although the NT inhibitory activity of dilazep is well documented, the nature of the interaction of dilazep with NT polypeptides remains unclear. In the present study, [^{3}H]dilazep was employed to explore the interactions of the NT inhibitor with S49 cells. NT in these cells occurs mainly through an equilibrative system of high sensitivity to NBMPR (5, 12, 14) [IC_{50} for inhibition of adenosine uptake, 1.7 nM (20)] although, in a recent study, about 10% of thymidine transport capacity

This work was supported by the Alberta Heritage Savings Trust Fund - Applied Research, Cancer, the Medical Research Council of Canada, and the National Cancer Institute of Canada. A.R.P.P. is a Senior Research Scientist of the National Cancer Institute of Canada.

ABBREVIATIONS: NT, nucleoside transport; FMT, Fischer's medium without serum or bicarbonate, containing 20 mM *N*-2-hydroxyethylpiperazine-*N'*-2-ethanesulfonic acid at specified pH values; NBMPR (nitrobenzylthioinosine), 6-[(4-nitrobenzyl)thio]-9-β-D-ribofuranosylpurine.

in S49 cells was of low sensitivity to NBMPR (29). Dilazep inhibited adenosine transport in S49 cells, with an IC_{50} value of 8 nM (20).

This study demonstrates (i) the pH dependence of high affinity, site-specific binding of dilazep in S49 cells and (ii) the interaction of protonated and nonprotonated forms of the drug at separate binding sites. An analysis of rates of dissociation of dilazep from sites on S49 cells in the presence of dilazep and NBMPR suggests that sites for the nonprotonated form of dilazep overlap with NBMPR sites.

Experimental Procedures

Materials. [G-^{3}H]Dilazep (20 Ci/mmol) and [G-^{3}H]NBMPR (16 Ci/mmol) were from Moravek Biochemicals (Brea, CA). [^{3}H]Dilazep was purified by high performance liquid chromatography using a C_{18} reverse phase column eluted with a linear gradient of 0–15% phosphate-buffered KCl (10 mM KH_2PO_4, 500 mM KCl) in 70% aqueous methanol. [^{3}H]NBMPR was purified by high performance liquid chromatography using the same column eluted with a linear gradient of 0–25% methanol in water. Dilazep dihydrochloride was generously provided by Hoffmann-La Roche & Co. (Basel, Switzerland). Concentrations of dilazep dihydrochloride in aqueous solutions were determined spectrophotometrically (E_{266} = 18,420). Hexobendine was a gift from Chemie Linz AG (Linz, Austria). Physostigmine (99%) was from Aldrich Chemical Company (Milwaukee, WI). NBMPR was synthesized in this laboratory (30). 9-β-D-Arabinosylcytosine was a gift from the Division of Cancer Treatment, National Cancer Institute (Bethesda, MD). S49 mouse lymphoma cells and AE_1 cells [an NT-deficient S49 mutant line (31)] were maintained in Fischer's medium (GIBCO Canada, Burlington, Ontario) with 10% horse serum.

Equilibrium binding experiments. S49 or AE_1 cells, harvested during exponential growth, were resuspended in FMT. Cells (1–3 × 10^6) were incubated for 30 min at 22° in FMT (total volume, 1 ml) that contained graded concentrations of [^{3}H]dilazep or [^{3}H]NBMPR. Nonspecific binding was determined in the presence of the same nonradioactive ligand (5 μM). In most experiments, cells were suspended in ligand-containing FMT layered over 100 μl of a silicone oil/paraffin oil solution (density, 1.03 g/ml) and, to end incubation intervals, cells were pelleted centrifugally (16,000 × *g*, 30 sec) under the oil. Free ligand was determined by measurement of radioactivity in samples of supernatant. Bound ligand (pellet-associated radioactivity) was determined in cell pellets dissolved in 5% Triton X-100. Radioactivity was measured in the presence of a Triton X-100-based scintillant (32). Site-specific binding of ligand (site-bound radioactivity) was determined as the difference between total pellet-associated radioactivity and that measured in the presence of 5 μM nonradioactive ligand. In each experiment shown, data points are the mean values of triplicate determinations. Mass analysis of equilibrium binding data, according to the method of Scatchard, was performed with the computer program LIGAND (33).

In the experiment of Fig. 1, the oil layer was omitted and nonspecific binding was determined in the presence of 2 μM nonradioactive dilazep. Residual supernatant was removed from cell pellets by aspiration. This procedure yielded results that were equivalent to those obtained in the oil-centrifugation procedure.

Kinetics of dilazep-site association and dissociation. Cells were suspended in FMT, pH 7.4, at 22°. Intervals of ligand-site association were initiated by the addition of cell suspensions (0.5 ml of FMT containing 1.9 × 10^6 cells) to 0.5-ml portions of FMT, containing 4 nM [^{3}H]dilazep, that were layered over 100 μl of oil in microcentrifuge tubes. Assay tubes (two to nine replicates) were prepared for each time point on the association time course. Nonspecific binding was determined in samples that contained 5 μM nonradioactive dilazep. Intervals of ligand-site association were ended by pelleting the cells under the oil layer. Bound (pellet-associated) radioactivity was determined as in equilibrium binding experiments.

Ligand-site dissociation time courses were obtained by preparing triplicate 1-ml mixtures that contained 2 nM [^{3}H]dilazep and 1.5–2.0 × 10^6 cells, as in association experiments. Site-bound and free ^{3}H-ligand reached equilibrium in 30 min at 22°, after which the association reaction was eliminated by the rapid addition (in 50 μl of water) of 2 μM nonisotopic dilazep, to block rebinding of [^{3}H]dilazep molecules, or nonisotopic nucleosides, to perturb the [^{3}H]dilazep-site equilibrium. After appropriate intervals, cells were pelleted under the oil and pellet ^{3}H content was measured. The addition of 50 μl of water did not measurably affect the ligand-site equilibrium. Dissociation data shown in Results were plotted as first-order reactions, according to the rate equation,

$$\ln B_t / B_0 = -k_{-1}\, t \qquad (1)$$

In this expression, B_t is the number of [^{3}H]dilazep molecules specifically bound at time t, B_0 is the number bound at equilibrium (time 0), and k_{-1} is the dissociation rate constant.

Values for dissociation rate constants were estimated using the computer program KINETIC (34), in which a weighted, nonlinear, curve-fitting technique allows comparison of fits of the data to either a monoexponential (one-site) or biexponential (two-site) model.

Chromatographic identification of cell-associated [^{3}H]dilazep. S49 cells (1 × 10^6/ml) were incubated with 2.5 nM [^{3}H]dilazep in FMT, pH 7.4, at 22°. Physostigmine (20 μM), an esterase inhibitor, was included in some samples. After 30 min, cell pellets were extracted with 20 μl of ice-cold methanol and portions of the extracts were chromatographed on silica gel G thin layer sheets [Brinkmann Instruments (Canada) Ltd., Rexdale, Ontario] that were developed in chloroform/methanol, 85:15 (v/v) (R_f for dilazep, 0.66). Radioactivity was measured in 1-mm slices of the chromatograms.

Results

Site-specific binding of dilazep under equilibrium conditions. Fig. 1 shows the relationship of cell-associated and free [^{3}H]dilazep after equilibration at pH 7.4 with S49 cells and with AE_1 cells, a line derived from an NT-deficient S49 mutant clone (31) that lacks high affinity binding sites for NBMPR (35). Binding of the ligand to S49 cells included both a nonsaturable component (about 20% of total bound ligand at 1 nM free ligand concentrations) and a saturable component that represented site-specific binding. In AE_1 cells, site-specific binding was not apparent.

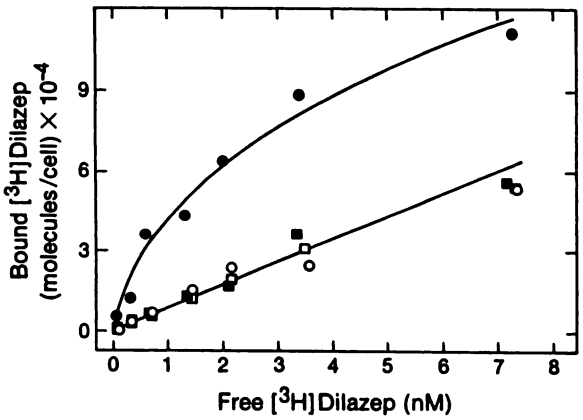

Fig. 1. Equilibrium binding of [^{3}H]dilazep to S49 (*circles*) and AE_1 (*squares*) cells. Cells were incubated with the ligand at pH 7.4 for 30 min in the absence (*filled symbols*) or presence (*open symbols*) of 2 μM nonradioactive dilazep. These conditions provided a determination of total and nonspecific binding, respectively.

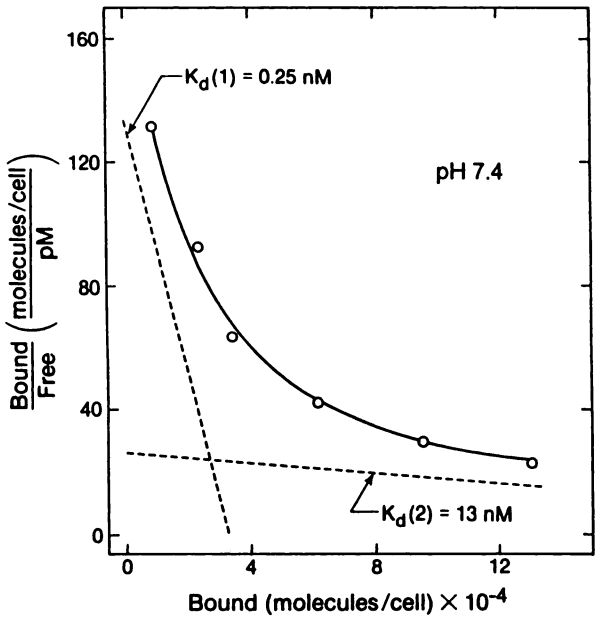

Fig. 2. Mass law (Scatchard) analysis of [^{3}H]dilazep binding to S49 cells at pH 7.4. The curvilinear plot was resolved into two components (– – –) using the computer program LIGAND (33), yielding constants for ligand binding at two populations of sites. In the experiment shown, B_{max} values for sites 1 and 2 were 3.3 × 10^4 molecules/cell and 3.4 × 10^5 molecules/cell, respectively.

Mass law analysis of data for site-specific binding of [^{3}H] dilazep to S49 cells at pH 7.4 is shown in Fig. 2. The curvilinear plot is taken to be the resultant of two components of binding, representing dilazep interaction with sites of two classes that differed about 50-fold in affinity for dilazep. Data from this experiment and three similar experiments showed that dilazep site densities for the high affinity binding component [3.0 ± 0.4 × 10^4 molecules/cell; K_d, 0.21 ± 0.04 nM (mean ± SE)] approximated site densities for NBMPR (about 6 × 10^4 molecules/cell; see below), whereas site densities for the low affinity component of dilazep binding (K_d, 10 ± 3 nM) were 3.5 ± 0.7 × 10^5 molecules/cell. Constants for dilazep binding at the latter sites are poor estimates because the highest ligand concentration used in these experiments was similar to the K_d value at the low affinity sites. The ligand concentrations employed were, however, sufficient to explore for the presence of both high and low affinity sites in the AE_1 cells (Fig. 1), because low affinity sites (K_d, 16 nM) were detected at similar free ligand concentrations in Novikoff UA cells, which lack high affinity binding sites for dilazep.[1]

Identification of cell-associated ^{3}H as nonmetabolized [^{3}H]dilazep. Thin layer chromatography of methanol extracts from S49 cells following incubation with [^{3}H]dilazep (30 min, 22°) showed that >95% of the applied ^{3}H was in the form of dilazep (data not shown). When physostigmine was included in the incubation mixtures, similar results were obtained. Thus, cell-associated radioactivity measured after equilibration of cells and ligand was in the form of dilazep, and metabolites of the ligand were not evident. It is, therefore, unlikely that the nonlinearity of Scatchard plots reflected binding of dilazep metabolites.

[1] W. P. Gati and A. R. P. Paterson, unpublished results.

pH dependence of dilazep binding under equilibrium conditions. When S49 cells were incubated with 2 nM [^{3}H] dilazep at pH values between 5 and 9, site-specific binding of the ligand increased with pH (Fig. 3A), as did the fraction of nonprotonated dilazep molecules [pK_a values for dilazep are 5.2 and 8.9 (24)]. It is noteworthy that site-specific binding of dilazep was significant at pH 5.3, under which condition >99% of dilazep molecules would be protonated. In a similar experiment, binding of 0.5 nM [^{3}H]NBMPR, a nonionized NT inhibitor at physiological pH values, was affected only slightly by changes in pH between 5 and 9 (Fig. 3B), indicating that NBMPR binding sites were not altered significantly by such changes in pH. If high affinity dilazep sites and NBMPR sites have in common the determinants for dilazep binding (see below), these results would appear to exclude pH effects on binding sites as a basis for the observed pH dependence of [^{3}H] dilazep binding.

Fig. 4 presents mass law analyses of site-specific [^{3}H]dilazep binding at pH 5.0 and pH 9.0. At pH 5.0 (>99% of dilazep molecules were protonated), only the low affinity binding component was evident, whereas, at pH 9.0 (43% of dilazep molecules were protonated), the high affinity binding component predominated. Data from this experiment and two similar experiments at pH 5.0 yielded, for the low affinity binding

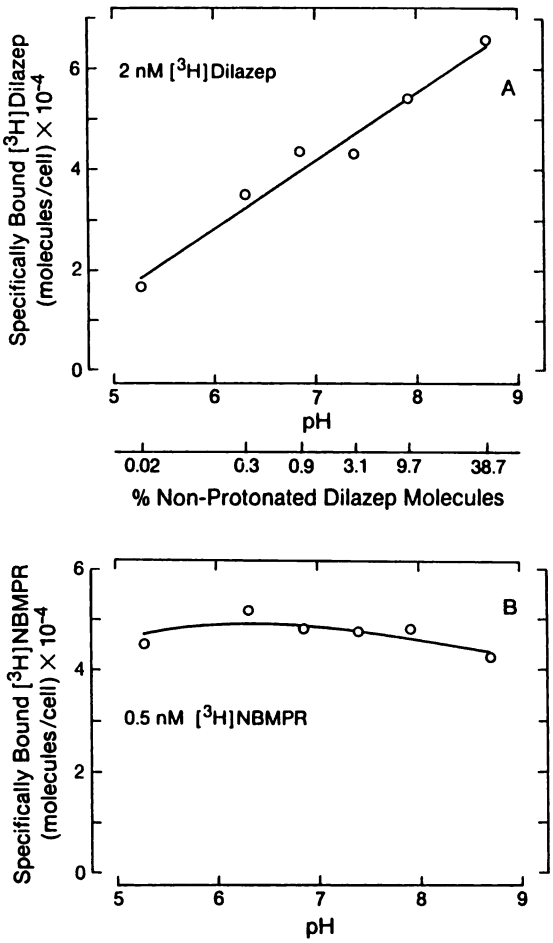

Fig. 3. pH dependence of specific binding of [^{3}H]dilazep (A) and [^{3}H] NBMPR (B) to S49 cells at equilibrium. Cells were incubated with 2 nM [^{3}H]dilazep or 0.5 nM [^{3}H]NBMPR. Nonspecific binding was determined in the presence of 5 μM concentrations of the respective nonradioactive ligands.

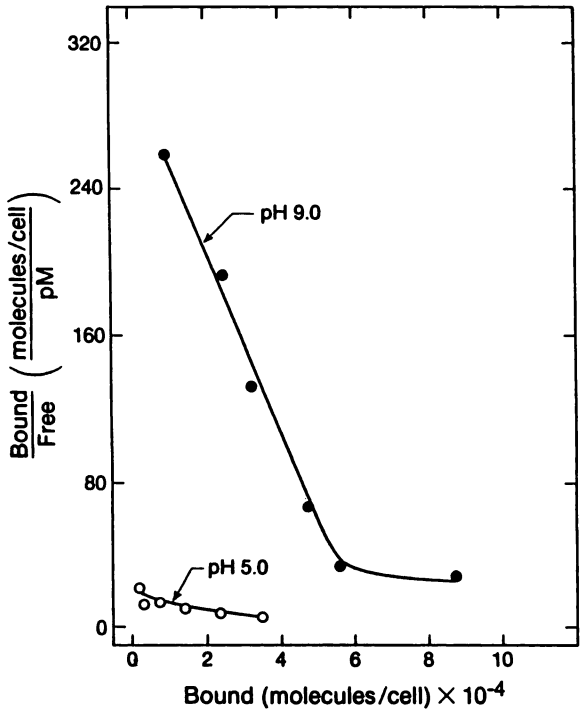

Fig. 4. Mass law (Scatchard) analysis of [^{3}H]dilazep binding to S49 cells at pH 5.0 and 9.0. Constants for the predominant binding components at each pH were determined using the program LIGAND (33). At pH 9.0: K_d, 0.16 nM; B_{max}, 4.9 × 10^4 molecules/cell. At pH 5.0: K_d, 3.1 nM; B_{max}, 4.4 × 10^4 molecules/cell.

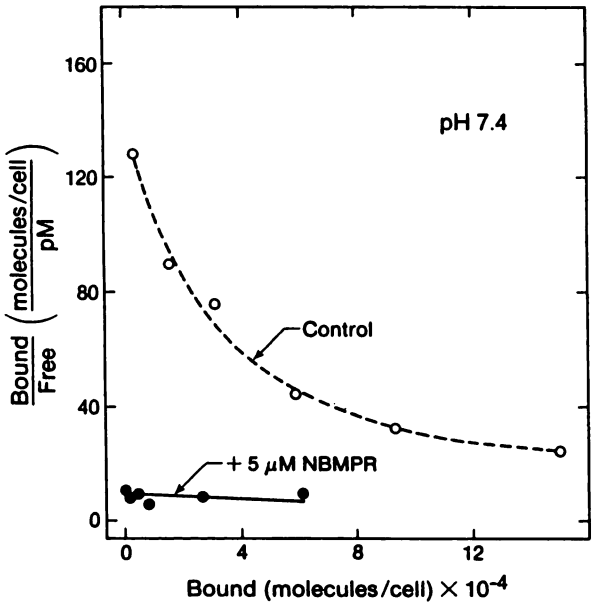

Fig. 5. Mass law (Scatchard) analysis of [^{3}H]dilazep binding to S49 cells at pH 7.4 in the absence (*Control*) and presence of 5 μM concentrations of NBMPR.

component, q K_d value of 33 ± 16 nM and q B_{max} value of 3.3 ± 1.6 × 10^5 molecules/cell (mean ± SE). Similarly, at pH 9.0, constants obtained for the high affinity binding component were q K_d value of 0.24 ± 0.08 nM and q B_{max} value of 5.9 ± 1.7 × 10^4 molecules/cell. Thus, at acidic pH values, dilazep binding apparently resulted from interaction of protonated dilazep molecules at sites with a low affinity for the ligand, whereas, at alkaline pH values, interaction of nonprotonated dilazep molecules at high affinity sites predominated. These results suggest that the curved Scatchard plot of Fig. 2 was the resultant of two components of dilazep binding that reflect the interactions of protonated and nonprotonated dilazep molecules at separate sites on NT-associated polypeptides.

Inhibition of site-specific binding of dilazep by NBMPR and physostigmine. In the experiment of Fig. 5, equilibrium binding of [^{3}H]dilazep was measured at pH 7.4 (a condition under which both high and low affinity components of binding are evident) in the absence and in the presence of NBMPR. Fig. 5 shows that the high affinity component of dilazep binding was abolished in the presence of 5 μM NBMPR, a concentration sufficient to saturate NBMPR binding sites in the S49 cells. The low affinity component of dilazep binding persisted in the presence of NBMPR.

Equilibrium binding of [^{3}H]NBMPR in S49 cells (data not shown) revealed a single binding component, with constants (K_d, 0.092 nM, B_{max}, 6.3 × 10^4 molecules/cell) that were similar to previously reported values (35, 36). Inhibition of [^{3}H]NBMPR binding by dilazep and hexobendine was competitive, inasmuch as the apparent K_d value for site-bound [^{3}H]NBMPR varied while B_{max} values did not change in the presence of the inhibitors. Apparent K_i values for the inhibition of NBMPR binding by dilazep and hexobendine were 1.7 and 16 nM, respectively, values based on the initial concentrations of the inhibitors in the incubation mixtures. In separate experiments (data not shown), depletion of 0.125–20 nM [^{3}H]dilazep in such incubation mixtures was 40–60% as a result of partitioning of dilazep into oil layers and association with cells. Thus, depletion-corrected K_i values for the inhibition of NBMPR binding by dilazep and hexobendine might be about one half of the above values. Others have reported inhibition by dilazep and hexobendine of NBMPR binding by human erythrocytes [K_i values of 0.3 and 1.9 nM, respectively (26)] and inhibition by dilazep of NBMPR binding by hamster fibroblasts [K_i values of 15–32 nM (27)].

Fig. 6 shows that, in the presence of 20 μM physostigmine, which is 75% protonated at pH 7.4 [pK_a values of 1.8 and 7.9 (37)], the low affinity component of dilazep binding was substantially reduced, whereas the K_d value (0.62 nM) for the high affinity component of dilazep binding was unchanged under these conditions. In a similar experiment (data not shown), the low affinity component of dilazep binding was reduced only slightly in the presence of 10 μM physostigmine at pH 8.5 (19% of physostigmine molecules protonated). These effects of physostigmine did not represent inhibition of esterase activity, because separate experiments (see above) showed that cell-associated ^{3}H was exclusively in the form of dilazep, either in the presence or absence of physostigmine. The concentrations of protonated physostigmine present at pH 7.4 and 8.5 (15 and 2 μM, respectively) indicate that the protonated species of physostigmine was responsible for inhibition of the low affinity component of dilazep binding. Similarly, the effective concentration of nonprotonated physostigmine in the experiment at pH 7.4 (5 μM) was less than that in the experiment at pH 8.5 (8 μM), although inhibition of the low affinity dilazep binding component was less in the latter experiment. These results further support the concept that the low affinity component of dilazep binding represented the interaction of protonated dilazep molecules.

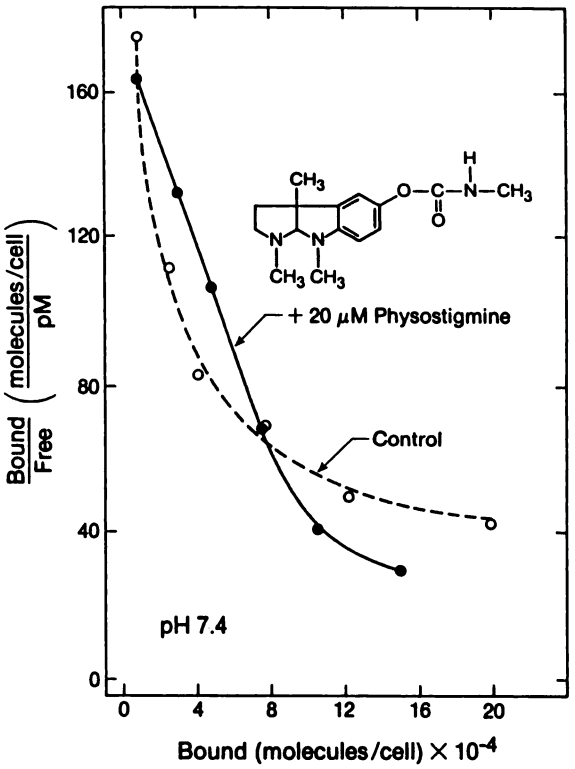

Fig. 6. Mass law (Scatchard) analysis of [^{3}H]dilazep binding to S49 cells at pH 7.4 in the absence (control) and presence of 20 μM concentrations of physostigmine.

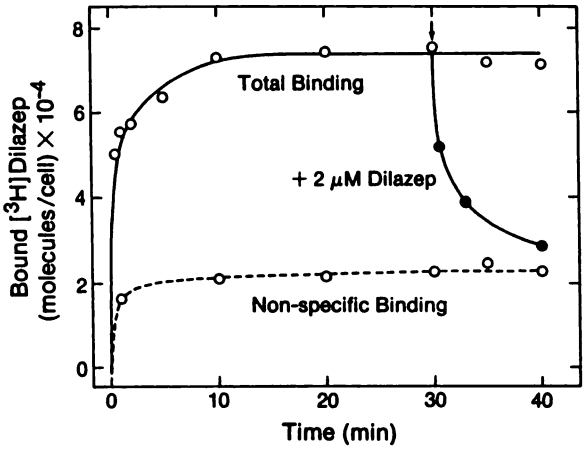

Fig. 7. Time courses of the association and dissociation of [^{3}H]dilazep from sites on S49 cells at pH 7.4. Cells were incubated with 2 nM concentrations of the ligand. Bound ligand was measured after graded time intervals, as described in Experimental Procedures. Nonspecific binding was determined in the presence of 5 μM concentrations of nonradioactive dilazep. Dissociation of the site-bound radioactive ligand was measured after addition (*arrow*) of 2 μM nonradioactive dilazep, a concentration sufficient to prevent reassociation of the radioactive ligand.

The experiments of Figs. 5 and 6 show that NBMPR and physostigmine each selectively inhibited one of the two components of dilazep binding and that inhibition of binding of either nonprotonated or protonated species of dilazep yielded Scatchard plots resembling those obtained at pH 5.0 and 9.0, respectively (Fig. 4).

Kinetics of dilazep association and dissociation. Fig. 7 shows a time course (22°, pH 7.4) for the association of 2 nM [^{3}H]dilazep with sites on S49 cells. Equilibrium between ligand and binding sites was reached after 15 min under these conditions. Addition to the equilibrium mixture of 2 μM nonradioactive dilazep resulted in rapid dissociation of the site-bound ^{3}H-ligand, demonstrating reversibility of dilazep binding; presumably, the presence of the nonradioactive ligand prevented rebinding of released [^{3}H]dilazep molecules.

Computer-assisted analysis (34) of [^{3}H]dilazep-site dissociation time courses in the presence of 2 μM nonradioactive dilazep (data not shown) revealed two components of dissociation, an initial rapid component (k_{-12}, 3.4–4.7 min^{-1}) and a second slower component (k_{-11}, 0.13–0.15 min^{-1}). These components likely describe dilazep dissociation from the low and high affinity sites. The nonlinearity of these plots would appear to exclude binding at a single class of sites; in such a system, data for dissociation measured in the presence of a high concentration of nonradioactive ligand would be linear when plotted according to Eq. 1 (for a discussion of this concept, see Ref. 38). This result supports the view that the nonlinear Scatchard plots obtained under equilibrium conditions (Figs. 2, 5, and 6) resulted from the binding of two species of ligand at separate sites and did not represent negative cooperativity in binding at a single site.

When [^{3}H]dilazep dissociation rates were measured in the presence of NBMPR (Fig. 8), the initial rapid component of dissociation described above (k_{-12}, 3.4–4.7 min^{-1}) was not apparent, suggesting that NBMPR did not interact at the low affinity dilazep binding sites. Furthermore, dissociation of dilazep molecules in the presence of NBMPR was incomplete, reaching about 70% after a 10-min exposure to 2 μM NBMPR.

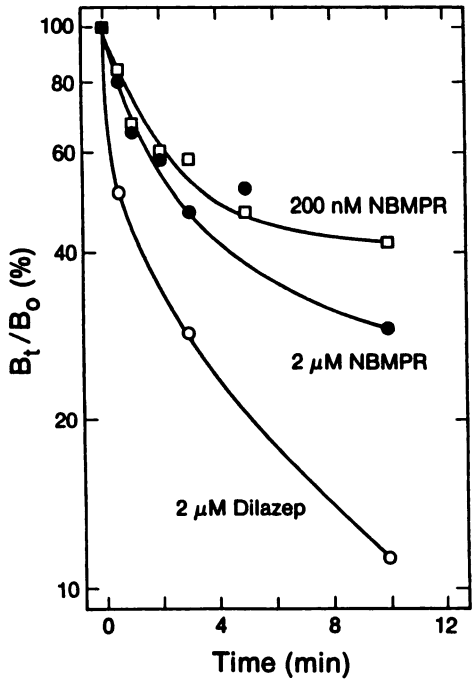

Fig. 8. Time courses of the dissociation of [^{3}H]dilazep from sites on S49 cells at pH 7.4 in the presence of nonradioactive dilazep or NBMPR. Cells were incubated with 2 nM concentrations of the radioactive ligand. After 30 min (time 0), excess nonradioactive dilazep (2 μM) or NBMPR (200 nM or 2 μM) was added to block rebinding of [^{3}H]dilazep molecules. Bound ligand was measured after graded time intervals as described in Experimental Procedures. Plotted are measures of specifically bound [^{3}H]dilazep at each time, according to Eq. 1.

The dissociation curve in the presence of 200 nM NBMPR was complex and appeared to fit a two-site model with rate constants k_{-11}, 0.04 and k_{-12}, 1.2 min^{-1}. However, those values did not correspond to rate constants for dissociation from either the high or low affinity sites in the presence of 2 μM dilazep. In the presence of 2 μM NBMPR, the dissociation curve yielded a single rate constant (0.11 min^{-1}), similar to that for dissociation of dilazep from high affinity sites in the presence of 2 μM nonradioactive dilazep. This result is consistent with the observation (Fig. 5) that 5 μM NBMPR inhibited binding of [^{3}H]dilazep at the high affinity sites under equilibrium conditions.

In the presence of 2 μM nonradioactive dilazep plus NBMPR (200 nM or 2 μM), time courses of [^{3}H]dilazep dissociation were indistinguishable from those obtained in the presence of 2 μM nonradioactive dilazep alone (data not shown). Thus, although dissociation of [^{3}H]dilazep from high affinity sites occurred in the presence of NBMPR alone (Fig. 8), the latter did not affect rates of dilazep dissociation from either high or low affinity sites measured in the presence of excess nonradioactive dilazep. These data suggest that NBMPR interacted at high affinity dilazep binding sites and not at separate allosteric sites.

Dissociation of site-bound [^{3}H]dilazep occurred also in the presence of the nucleoside permeants uridine, arabinosylcytosine, and 2′-deoxyadenosine (Fig. 9), although the rapid component of dissociation was absent and dissociation was incomplete. Whereas dissociation in the presence of 2 mM uridine was slight, rate constants for the single component of dissociation that was identified in the presence of 10 mM uridine (k_{-11}, 0.13 min^{-1}), 2.9 mM arabinosylcytosine (k_{-11}, 0.16 min^{-1}), and 470 μM 2′-deoxyadenosine (k_{-11}, 0.19 min^{-1}) were similar to the rate constant for dissociation of [^{3}H]dilazep from high affinity sites that was measured in the presence of 2 μM nonradiaoctive dilazep. These results suggest that the nucleoside permeants interfered with the binding of dilazep at high affinity sites, yielding results similar to those obtained in the presence of NBMPR.

Discussion

Results of this study are consistent with a model in which [^{3}H]dilazep binds at two populations of sites on S49 cells. Neither binding component was detected on AE_1 cells, a mutant line of S49 cells that is NT-deficient (31, 39) and lacks high affinity binding sites for NBMPR (35), suggesting that in S49 cells site-specific binding of dilazep occurred primarily at NT-associated sites.

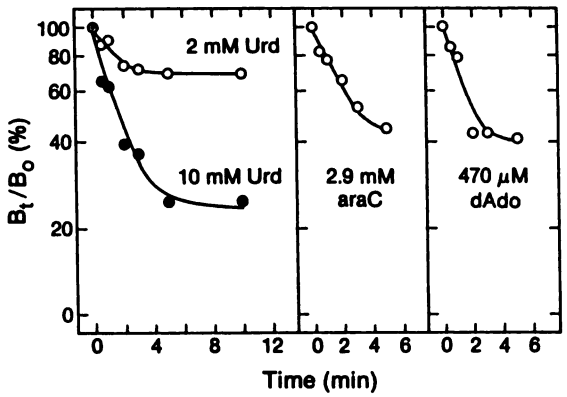

Fig. 9. Time courses of the dissociation of [^{3}H]dilazep from sites on S49 cells at pH 7.4 in the presence of the nucleoside permeants uridine (*Urd*), arabinosylcytosine (*araC*), and 2′-deoxyadenosine (*dAdo*). Dissociation was measured as described in the legend to Fig. 8. The data are plotted according to Eq. 1.

Mass law analysis of equilibrium binding of dilazep to S49 cells yielded curvilinear Scatchard plots, a result that might be attributable to (i) negative cooperativity of the ligand binding at a single population of sites, (ii) binding of both ligand and metabolites of the ligand, or (iii) the presence of more than one population of binding sites. The first two possibilities were inconsistent with (i) dissociation kinetics of [^{3}H]dilazep and (ii) the identity of cell-associated radioactivity after incubation with the ligand. On the other hand, the third possibility was supported by the observation that both protonated and nonprotonated species of dilazep were present and the observation that binding of the ligand was pH dependent. The results suggest that curvilinear Scatchard plots resulted from the interactions of protonated and nonprotonated molecules of dilazep at separate sites, which have affinities that differed about 50-fold. This hypothesis was supported in three ways, (i) computer-assisted curve peeling in the mass law analysis of equilibrium binding data, which was consistent with a two-site model; (ii) selective reduction of the concentration of either protonated or nonprotonated species of dilazep in solution through changes in pH, resulting in substantial reduction of one of the respective binding components in each instance; and (iii) selective blocking of either of the two sites through the use of competing ligands, so that one of the components of binding was significantly reduced or eliminated in each case.

This study suggests that protonated dilazep molecules interacted at the low affinity sites and that such binding was inhibited by protonated physostigmine molecules. Nonprotonated dilazep molecules appeared to interact at high affinity sites identical to, or overlapping with, NBMPR binding sites, because (i) inhibition of [^{3}H]NBMPR binding by dilazep appeared to be competitive, (ii) concentrations of NBMPR sufficient to saturate sites for the latter eliminated the high affinity dilazep binding component under equilibrium conditions, (iii) dissociation of [^{3}H]dilazep from high affinity binding sites occurred in the presence of NBMPR, and (iv) the rate of dissociation of [^{3}H]dilazep from binding sites in the presence of nonradioactive dilazep was not altered by the additional presence of NBMPR.

Other investigators have shown that the addition of micromolar concentrations of dilazep together with NBMPR decreased the rate of NBMPR-induced dissociation of [^{3}H]NBMPR from sites on hamster fibroblasts (27) and human erythrocytes and P388 cells (23). Those studies suggested that dilazep interacted at sites distinct from NBMPR sites on those cells. The present results are not inconsistent with such an hypothesis, because they show that protonated dilazep molecules, the most abundant species of dilazep under the pH conditions of the [^{3}H]NBMPR dissociation experiments, interact at low affinity sites that are apparently distinct from NBMPR sites. It is possible that protonated dilazep molecules may cause dissociation of NBMPR-site complexes by allosteric reduction of the affinity of the NBMPR binding site for that ligand.

In the present study, incomplete dissociation of [^{3}H]dilazep from sites on S49 cells was observed in the presence of arabinosylcytosine, 2′-deoxyadenosine, and uridine, suggesting that the permeants interacted at the high affinity sites. However, these effects occurred at high concentrations (0.5–10 mM) of the nucleosides and may be the result of nonspecific interac-

tions with membrane components. Others have shown that acceleration by uridine or adenosine of the dissociation of NBMPR from sites on human erythrocyte membranes was not saturable, concluding that these effects may have been nonspecific consequences of the high concentrations (0.5–20 mM) of the nucleosides used (40). In the present study, nucleoside effects on dilazep dissociation rates are difficult to interpret because cellular metabolism of the nucleosides may well have reduced their concentrations in the medium. Permeant entry would be substantial in these experiments, because 2 nM concentrations of dilazep in equilibrium with the S49 cells would inhibit only about 20% of permeant influx [IC_{50} for inhibition of adenosine influx, 8 nM dilazep (20)]. The present study does not provide evidence for identity of dilazep binding sites and nucleoside permeant binding sites.

This study suggests a model for dilazep interaction with S49 cells that includes two populations of binding sites, both associated with NT polypeptides. NBMPR sites appear to overlap dilazep sites of one type, because NBMPR only partially inhibits dilazep binding under equilibrium conditions and induces only partial dissociation of site-bound dilazep molecules. Dilazep, on the other hand, may elicit a virtually complete dissociation of NBMPR (27). Although the binding site density for the low affinity component of dilazep binding appears to be severalfold greater than that of the high affinity component, our estimates for the former component have the qualification that ligand concentrations were not sufficiently high in the assays used. The two populations of sites at which nonprotonated and protonated dilazep molecules are bound may be present on a single membrane protein, because neither binding component was detectable in AE_1 cells, an S49 mutant isolated by a single-step selection procedure (31).

Although this study has demonstrated site-specific binding of both protonated and nonprotonated dilazep molecules, the attribution of transport-inhibitory effects to the site interactions of one or both species remains to be examined.

Acknowledgments

The technical assistance of Jadwiga Kaleta and Herta Unger is gratefully acknowledged.

References

1. Paterson, A. R. P., and C. E. Cass. Transport of nucleoside drugs in animal cells, in *Membrane Transport of Antineoplastic Agents, International Encyclopedia of Pharmacology and Therapeutics, Section 118* (I. D. Goldman, ed.). Pergamon Press, Oxford, 309–329 (1986).
2. Paterson, A. R. P., E. S. Jakobs, C. Y. C. Ng, R. D. Odegard, and A. A. Adjei. Nucleoside transport inhibition *in vitro* and *in vivo*, in *Topics and Perspectives in Adenosine Research* (E. Gerlach and B. F. Becker, eds.). Springer-Verlag, Berlin Heidelberg, 89–101 (1987).
3. Young, J. D., and S. M. Jarvis. Nucleoside transport in animal cells. *Biosci. Rep.* **3**:309–322 (1983).
4. Plagemann, P. G. W., and R. M. Wohlhueter. Permeation of nucleosides, nucleic acid bases, and nucleotides in animal cells. *Curr. Top. Membr. Transp.* **14**:225–330 (1980).
5. Belt, J. A. Heterogeneity of nucleoside transport in mammalian cells: two types of transport activity in L1210 and other cultured neoplastic cells. *Mol. Pharmacol.* **24**:479–484 (1983).
6. Ungemach, F. R., and D. Hegner. Uptake of thymidine into isolated rat hepatocytes: evidence for two transport systems. *Hoppe-Seyler's Z. Physiol. Chem.* **359**:845–856 (1978).
7. Schwenk, M., E. Hegazy, and V. Lopez del Pino. Uridine uptake by isolated intestinal epithelial cells of guinea pig. *Biochim. Biophys. Acta* **805**:370–374 (1984).
8. Spector, R., and S. Huntoon. Specificity and sodium dependence of the active nucleoside transport system in choroid plexus. *J. Neurochem.* **42**:1048–1052 (1984).
9. Jakobs, E. S., and A. R. P. Paterson. Sodium-dependent, concentrative nucleoside transport in cultured intestinal epithelial cells. *Biochem. Biophys. Res. Commun.* **140**:1028–1035 (1986).
10. Darnowski, J. W., C. Holdridge, and R. E. Handschumacher. Concentrative uridine transport by murine splenocytes: kinetics, substrate specificity, and sodium dependency. *Cancer Res.* **47**:2614–2619 (1987).
11. Dagnino, L., L. L. Bennett, and A. R. P. Paterson. Concentrative transport of nucleosides in L1210 mouse leukemia cells. *Proc. Am. Assoc. Cancer Res.* **28**:15 (1987).
12. Plagemann, P. G. W., and R. M. Wohlhueter. Nucleoside transport in cultured mammalian cells: multiple forms with different sensitivity to inhibition by nitrobenzylthioinosine or hypoxanthine. *Biochim. Biophys. Acta* **773**:39–52 (1984).
13. Belt, J. A., and L. D. Noel. Nucleoside transport in Walker 256 rat carcinosarcoma and S49 mouse lymphoma cells: differences in sensitivity to nitrobenzylthioinosine and thiol reagents. *Biochem. J.* **232**:681–688 (1985).
14. Gati, W. P., J. A. Belt, E. S. Jakobs, J. D. Young, S. M. Jarvis, and A. R. P. Paterson. Photoaffinity labelling of a nitrobenzylthioinosine-binding polypeptide from cultured Novikoff hepatoma cells. *Biochem. J.* **236**:665–670 (1986).
15. Jarvis, S. M., and J. D. Young. Nucleoside transport in rat erythrocytes: two components with differences in sensitivity to inhibition by nitrobenzylthioinosine and *p*-chloromercuriphenyl sulfonate. *J. Membr. Biol.* **93**:1–10 (1986).
16. Jarvis, S. M., D. McBride, and J. D. Young. Erythrocyte nucleoside transport: asymmetrical binding of nitrobenzylthioinosine to nucleoside permeation sites. *J. Physiol. (Lond.)* **324**:31–46 (1982).
17. Jarvis, S. M. Nitrobenzylthioinosine-sensitive nucleoside transport system: mechanism of inhibition by dipyridamole. *Mol. Pharmacol.* **30**:659–665 (1986).
18. Woffendin, C., and P. G. W. Plagemann. Nucleoside transporter of pig erythrocytes: kinetic properties, isolation and reaction with nitrobenzylthioinosine and dipyridamole. *Biochim. Biophys. Acta* **903**:18–30 (1987).
19. Paterson, A. R. P., E. Y. Lau, E. Dahlig, and C. E. Cass. A common basis for inhibition of nucleoside transport by dipyridamole and nitrobenzylthioinosine? *Mol. Pharmacol.* **18**:40–44 (1980).
20. Paterson, A. R. P., E. S. Jakobs, E. R. Harley, N.-W. Fu, M. J. Robins, and C. E. Cass. Inhibition of nucleoside transport, in *Regulatory Function of Adenosine* (R. M. Berne, T. W. Rall, and R. Rubio, eds.). Martinus Nijhoff Publishers, The Hague, 203–200 (1983).
21. Paterson, A. R. P., E. R. Harley, and C. E. Cass. Inward fluxes of adenosine in erythrocytes and cultured cells measured by a quenched-flow method. *Biochem. J.* **224**:1001–1008 (1984).
22. Mahony, W. B., and T. P. Zimmerman. An assay for inhibitors of nucleoside transport based upon the use of 5-[^{125}I]iodo-2′-deoxyuridine as permeant. *Anal. Biochem.* **154**:235–243 (1986).
23. Plagemann, P. G. W., and M. Kraupp. Inhibition of nucleoside and nucleobase transport and nitrobenzylthioinosine binding by dilazep and hexobendine. *Biochem. Pharmacol.* **35**:2559–2567 (1986).
24. Mannhold, R., R. Rodenkirchen, R. Bayer, and W. Haas. The importance of drug ionization for the action of calcium-antagonists and related compounds. *Arzneim.-Forsch/Drug Res.* **34**:407–409 (1984).
25. Jarvis, S. M., and J. D. Young. Nucleoside transport in human and sheep erythrocytes: evidence that nitrobenzylthioinosine binds specifically to functional nucleoside-transport sites. *Biochem. J.* **190**:377–383 (1980).
26. Hammond, J. R., and A. S. Clanachan. [^{3}H]Nitrobenzylthioinosine binding to guinea pig CNS nucleoside transport system: a pharmacological characterization. *J. Neurochem.* **43**:1582–1592 (1984).
27. Koren, R., C. E. Cass, and A. R. P. Paterson. The kinetics of dissociation of the inhibitor of nucleoside transport, nitrobenzylthioinosine, from the high-affinity binding sites of cultured hamster cells. *Biochem. J.* **216**:299–308 (1983).
28. Woffendin, C., and P. G. W. Plagemann. Interaction of [^{3}H]dipyridamole with the nucleoside transporters of human erythrocytes and cultured animal cells. *J. Membr. Biol.* **98**:89–100 (1987).
29. Plagemann, P. G. W., and R. M. Wohlhueter. S49 mouse lymphoma cells are deficient in hypoxanthine transport. *Biochim. Biophys. Acta* **855**:25–32 (1985).
30. Paul, B., M. F. Chen, and A. R. P. Paterson. Inhibitors of nucleoside transport: a structure-activity study using human erythrocytes. *J. Med. Chem.* **18**:968–973 (1975).
31. Cohen, A., B. Ullman, and D. W. Martin. Characterization of a mutant mouse lymphoma cell with deficient transport of purine and pyrimidine nucleosides. *J. Biol. Chem.* **254**:112–116 (1979).
32. Pande, S. V. Liquid scintillation counting of aqueous samples using Triton-containing scintillants. *Anal. Biochem.* **74**:25–34 (1976).
33. Munson, P. J., and D. Rodbard. LIGAND: a versatile computerized approach for characterization of ligand-binding systems. *Anal. Biochem.* **107**:220–239 (1980).
34. McPherson, G. A. Analysis of radioligand binding experiments: a collection of computer programs for the IBM PC. *J. Pharmacol. Methods* **14**:213–228 (1985).
35. Cass, C. E., N. Kolassa, Y. Uehara, E. Dahlig-Harley, E. R. Harley, and A. R. P. Paterson. Absence of binding sites for the transport inhibitor nitrobenzylthioinosine on nucleoside transport-deficient mouse lymphoma cells. *Biochim. Biophys. Acta* **649**:769–777 (1981).

36. Aronow, B., K. Allen, J. Patrick, and B. Ullman. Altered nucleoside transporters in mammalian cells selected for resistance to the physiological effects of inhibitors of nucleoside transport. *J. Biol. Chem.* **260**:6226–6233 (1985).
37. Martin, A. N., J. Swarbrick, and A. Cammarata. *Physical Pharmacy*, 2nd Ed. Lea and Febiger, Philadelphia, 195 (1969).
38. Limbird, L. E. *Cell Surface Receptors: A Short Course on Theory and Methods*. Martinus Nijhoff Publishing, Boston, 93 (1986).
39. Plagemann, P. G. W., and C. Woffendin. Residual nitrobenzylthioinosine-resistant nucleoside transport in a transport mutant (AE_1) of S49 murine T-lymphoma cells. *Mol. Cell. Biol.* **7**:160–165 (1987).
40. Jarvis, S. M., S. N. Janmohamed, and J. D. Young. Kinetics of nitrobenzylthioinosine binding to the human erythrocyte nucleoside transporter. *Biochem. J.* **216**:661–667 (1983).

Send reprint requests to: Dr. Wendy P. Gati, Cancer Research Group (McEachern Laboratory), 5-75 Medical Sciences Building, University of Alberta, Edmonton, Alberta, Canada T6G 2H7.